Study and Validation of Polyamine Metabolism-Related Marker Genes Predicting Prognosis and Immunotherapy Response for Breast Cancer

Xiliang Zhang[1], Hanjie Guo[2], Haitao Ma[1], Wei Tao[1], Xiaoqian Ma[2], Xiaolong Li[1], Weidong Xiao[1]

[1]Department of General Surgery, Xinqiao Hospital, Army Medical University, Chongqing, China

[2]School of Medicine, South China University of Technology, Guangzhou, China

Introduction. Breast cancer (BC) is one of the most commonly diagnosed aggressive malignancies among women, and it is also the second leading cause of cancer-related deaths in women. BC is a significant global health issue that remains challenging to address, and there is still a considerable unmet medical need. Early diagnosis and timely monitoring are critical for improving the prognosis of BC and addressing this pressing public health concern.

Methods. Univariate Cox regression analysis was performed on 59 polyamine metabolism-related genes(PMRGs), and prognostic PMRGs were selected for further analysis. TCGA-BC patients were divided into different subtypes based on prognostic related PMRGs, and the differences in cell infiltration, clinical features, survival and functional enrichment of different subtypes were analyzed. Patients' transcriptomic data were extracted from TCGA-BC to compare the differentially expressed genes (DEGs) between cancer and paracancer, and then intermingled with prognostic related PMRGs to obtain significantly different prognostic related PMRGs, and the final biomarker was obtained after LASSO

learning. The risk model of BC was constructed and verified. GSEA and GSVA enrichment analyses were performed for biomarkers in the high-low risk group using the “clusterProfiler” package. Genetic variation and CNV variation frequency were analyzed in different risk groups. Subsequently, we conducted predictions on the immune microenvironment and immunotherapy in both the high and low-risk groups. We analyzed the differential expression of immune checkpoints and utilized the CTD database to predict potential drugs specifically targeting BC. Finally, we constructed a nomogram and evaluated its diagnostic efficacy for BC.The expression of biomarkers was verified by RT-qPCR.

Results. First, 14 prognostic related PMRGS were obtained and PPI network was constructed. The expression profile of TCGA-BC was divided into C1 and C2 subtypes by unsupervised clustering method. Combined with clinical information, the analysis found significant survival differences between the two subtypes. The distribution of T cells CD8, T cells regulatory Tregs, T cells gamma delta, Monocytes, Macrophages M1 and Mast cells resting were different in two clusters. The intersection of 14 prognostic related PMRGs and DEGs was used to obtain 10 related genes, and finally 5 biomarkers were obtained that could be used as prognostic related biomarkers of BC by machine learning, namely *PSMD10*, *PSMD14*, *PSMD2*, *PSME1* and *PSME2*. It was also found that the high risk group had significantly shorter OS than the low risk group. It was found from the risk curve that the mortality rate of the high-risk group was higher. GSEA and GSVA enrichment results showed that genes in different risk groups were enriched in different signaling pathways. TMB analysis showed that there were differences in the TOP10 genes with high mutation frequency in different risk

group. *TNFSF15* and *TNFSF4* did not exhibit significant differences. However, significant variations were observed in the expression levels of the other genes in different risk group. In addition, a total of 252 drug molecules were predicted based on the 5 biomarkers. It was found that the risk score was an independent prognostic factor for BC patients and risk model in constructed nomogram had high accuracy for BC.Finally, RT-qPCR results showed that these 5 biomarkers were highly expressed in BC tissues.

Conclusion. We found five biomarkers in BC, namely *PSMD10*, *PSMD14*, *PSMD2*, *PSME1*, and *PSME2*.The constructed risk score model had a high accuracy in the prognosis assessment of BC, indicating that these 5 biomarker genes were crucial for the clinical diagnosis of BC.

Keyword. Breast cancer, biomarker, immune microenvironment, therapeutic target.

1. INTRODUCTION

Breast cancer (BC) is a prevalent form of cancer among women, constituting approximately 7-10% of all malignancies[1]. It is frequently associated with genetic factors and has a higher incidence rate in women aged between 40 and 60 years, as well as during the pre- and post-menopausal stages. BC primarily develops in the glandular epithelial tissue of the breast. Although it predominantly affects women, men also account for around 0.5 to 1 percent of all BC cases[2]. BC is the second deadliest form of cancer[3]. The risk of developing BC increases with age. BC can metastasize to other organs, including the bones, lungs, liver, and brain[4]. Currently,

the standard treatment approaches for BC consist of surgery, chemotherapy, targeted therapy, immunotherapy and other interventions[5]. However, despite the availability of these treatments, many patients experience disease recurrence and secondary metastasis. Advanced and metastatic BC remains a significant challenge, with a survival rate of approximately 2-4 years. Thus, early diagnosis and ongoing monitoring are critical to improving the prognosis for patients with BC.

Polyamines (PA) are small, positively charged alkyl amines that are ubiquitous in eukaryotes and prokaryotes and regulate the biological activities and functions of nucleic acids, proteins and phospholipids[6]. Polyamines exist in cells and are widely involved in physiological and pathological processes such as cell proliferation, growth and apoptosis[7]. The content of free polyamines in cells is low, so polyamine metabolism must be precisely regulated to maintain polyamine homeostasis, so as to ensure the normal function of cells.Polyamines can significantly impact the development of cells and contribute to various diseases in the body. Research has found that low levels of polyamines in cells can affect the proteins on the cell membrane, leading to immune inflammatory reactions. Conversely, an excessive amount of polyamines can also cause cells to become cancerous. As a result, an increasing number of researchers are exploring the role of polyamine metabolism in tumor development and progression. Researchers such as Coni S have found that the combination of polyamine metabolism and eIF5A inhibits the growth of colorectal cancer[8]. Novita Sari et al reported that polyamines may have a potential role in the prevention and treatment of cancer[9]. Kaminski L et al. found that PGC1α can inhibit

the aggressiveness of prostate cancer by inhibiting polyamine synthesis[10]. Mendez R et al. found that polyamine metabolism can be used as an indicator for the early detection of pancreatic cancer[11]. Numerous studies have demonstrated a close association between polyamine metabolism and tumor development. Alterations in polyamine metabolism may contribute to the development of various diseases, including cancer. Research has shown that polyamine accumulation is evident in tumor cells, tissues, and even in the urine or serum of cancer patients. Therefore, it is crucial to gain a deeper understanding of the role of polyamine metabolism in tumor development and identify key genes that regulate this process. This knowledge can assist in developing selective therapies that target polyamine metabolism in cancer cells, thereby offering a new direction for improving the early diagnosis and prognosis of BC patients.

Using bioinformatics, this study aimed to identify prognostic biomarkers associated with polyamine metabolism in BC at the transcriptome level. Through functional analysis and molecular mechanism studies, the role of polyamine metabolism in BC was elucidated, providing a valuable theoretical foundation for BC prognosis and clinical treatment. These findings also contribute to the exploration of novel therapeutic avenues in the management of BC.

2. MATERIALS AND METHODS

2.1 Collect data

RNA-seq count data, survival information, clinical features, somatic mutation data and CNV data for TCGA-BC were downloaded from the TCGA database (113 normal breast samples and 1,109 BC samples). Download 1,904 BC samples from the METABRIC database. A total of 59 PMRGs were collected from MSigDB database.

2.2 Acquisition of PMRGs associated with prognosis and PP network construction

In order to obtain PMRGs related to prognostic, “survival” package was used to perform univariate Cox regression analysis to analyze the influence of each gene on prognosis and screened out the PMRGs with $p<0.05$. Based on the obtained prognostic PMRGs, the PPI network was constructed via STRING online website.

2.3 Classification of TCGA-BC patients

For unsupervised cluster analysis, we utilized the “ConsensusClusterPlus” package. In addition, K-means method was employed to determine the optimal number of clusters, with 1000 iterations performed to ensure classification stability. We also utilized the Nbclust package to identify the most robust cluster number.

2.4 Screening and enrichment analysis of DEGs among clusters

The DEGs between the two subpopulations were analyzed by “limma” package to obtain differential genes of $|log2FC|>1$ and $p<0.05$. GO and KEGG annotation were conducted by “clusterProfiler” packagefor to screen out TOP5 entries of $p<0.05$.

2.5 Acquisition of prognostic biomarkers associated with BC

The transcriptome data of patients were extracted from TCGA-BC by “limma” package to compare DEGs between cancer and pan-cancer. The screening criteria were |log2FC| >0.5 and pvalue<0.05. Then, they were intersected with prognostic related PMRGs, and obtained prognostic related PMRGs with significantly difference. "ggplot2" and "pheatmap" were used to draw volcano plot, and heatmap respectively to show the expression of DEGs. Univariate Cox regression analysis was performed using “survival” and LASSO analysis using “glmnet” to obtain final prognostic biomarkers of BC.

2.6 Construction and verification of risk model

We constructed a risk model using following formula: Riskscore = (0.0045543358468217 8*PSMD10)+(0.0583273428343866*PSMD14)+(0.0059211185137735*PSMD2)+(0.0020321443275715 4*PSME1)+(-0.0231947567758718*PSME2). The “predict” package was used to predict the risk score of patients with BC, who were divided into a high risk group and a low risk group. Kaplan-Meier survival curves were plotted and "pROC" package was used to plot ROC curves for training sets and validation sets in 1, 2, and 3 years. Besides, plot risk curves for different risk groups were plotted.

2.7 GSEA and GSVA enrichment analysis

We conducted GSEA enrichment analysis for all genes in different group via “clusterProfiler” package. The threshold settings were defined as |NES| > 1, NOM p < 0.05, and q< 0.25. Furthermore, KEGG analysis was conducted using the "GSVA" package, with a p-value < 0.05 used as the criterion to identify significantly enriched

pathways.

2.8 Genetic variation analysis

We conducted a tumor mutation load (TMB) analysis using the "maftools" package, and mapped the mutations specific to BC in different risk groups. Additionally, we performed CNV mutation frequency analysis using GISTIC 2.0 and visualized the results using "maftools".

2.9 Immune microenvironment analysis

We employed the ssGSEA algorithm to compare the variances in immune cells across samples from different groups. Additionally, we utilized the ESTIMATE algorithm to assess proportions of stromal and immune cells in tumor samples. Finally, we analyzed and visualized the expression of immune checkpoints using violin diagram.

2.10 Prediction of potential drugs targeting BC

We performed individual searches for each biomarker using the CTD database. Subsequently, we constructed a biomarker-drug interaction network and identified chemotherapy drugs that could potentially modulate the expression levels of these biomarkers and utilized Cytoscape software for visual analysis.

2.11 Construction of a nomogram

In this study, we employed univariate and multivariate Cox regression analyses to assess whether the risk scores served as clinically independent prognostic factors for BC patients. Based on age, stage, and risk scores, we constructed a nomogram model via “survival” and “rms” packages. We further evaluated the accuracy of this

nomogram by conducting prognostic ROC analysis.

2.12 RT-qPCR

Seven cases of BC tissues and their corresponding adjacent tissues were collected. Total RNA was extracted using the Trizol method and reverse transcribed into cDNA. Subsequently, RT-qPCR was performed under the following conditions: initial denaturation at 95°C for 30 seconds, followed by cycling reactions at 95°C for 20 seconds, 60°C for 34 seconds, for a total of 40 cycles. A melting curve analysis was conducted from 60°C to 95°C with a temperature increment of 0.05°C/s. GAPDH was used as an internal reference control, and the results were analyzed using the 2^-△△Ct method.The sequence of primers was shown in Table 1.

2.13 Statistical analysis

All analyses in this study were conducted using R version 4.2.1. The Wilcoxon rank-sum test was employed to compare the differences between the two groups of samples. Statistical significance was considered at a level of $p<0.05$.

3. RESULTS

3.1 Differentiation of polyamine metabolic subtypes in BC

We performed analysis on 56 genes related to PMRGs, resulting in identification of 14 PMRGs that were significantly associated with prognosis and the finding was depicted in Figure 1A.Subsequently, we utilized the STRING website to construct PPI networks of 14 PMRGs that were associated with prognosis. The resulting network

was presented in Figure 1B, we observed that the remaining genes exhibited relatively complex interactions in PPI networks, with the exception of PAOX and AZIN.We used K-means to determine the optimal number of clusters, as demonstrated in Figure 1C-E. Through this analysis, we identified two distinct clusters, which we subsequently labeled as C1 and C2. We further integrated clinical information and compared the survival differences between these two clusters, ultimately discovering a significant survival disparity (p-value=0.0011,Figure 1F).Then we screened $p<0.05$ DEGs between the two clusters, and made GO and KEGG annotations, as shown in Figure 1G. Our analysis revealed the top 5 enriched GO pathways, which included OXIDATIVE PHOSPHORYLATION, PROTON MOTIVE FORCE DRIVEN ATP SYNTHESIS, AEROBIC RESPIRATION and NADH DEHYDROGENASE COMPLEX, RESPIRASOME, STRUCTURAL CONSTITUENT OF RIBOSOME, PRIMARY ACTIVE TRANSMEMBRANE TRANSPORTER ACTIVITY.The TOP5 KEGG pathways were RIBOSOME、PARKINSONS DISEASE、OXIDATIVE PHOSPHORYLATION、HUNTINGTONS DISEASE and ALZHEIMERS DISEASE. Finally, Figure 1H&I results revealed that distribution of inmmune cell such as T cells CD8, T cells follicular helper, T cells regulatory Tregs, T cells gamma delta, Monocytes, Macrophages M1 were significantly different in two clusters.

3.2 Identification of prognostic PMRGs in BC

Firstly,we screened for DEGs in the transcriptome data of BC and adjacent tissues from patients. The resulting DEGs were visualized through volcano plot and heatmap

respectively, as illustrated in Figure 2A&B. We then intersected these DEGs with the 14 PMRGs that were found to be prognostic related, ultimately identifying 10 PMRGs that displayed significant differences and corresponded to prognosis. These 10 genes included *PSME1*, *PSME2*, *PSMA7*, *PSMD10*, *PSMD14*, *AZIN1*, *PSMD2*, *PSMB8*, *PSMB10*, and *PSMB9*, as depicted in Figure 2C.Subsequently, a total of 5 biomarkers were obtained that could be used as prognostic markers of BC, namely *PSMD10*, *PSMD14*, *PSMD2*, *PSME1* and *PSME2*, as shown in Figure 2D-F.

3.3 Construction and verification of risk model

Kaplan-Meier survival curves results revealed that patients in the high-risk group exhibited significantly lower OS rates than those in low-risk group, as illustrated in Figure 3A&D.Subsequently, ROC curves were generated for the training set and validation sets at 1, 2, and 3 years based on the risk model. Figure 3B&E demonstrated that AUC values were generally around 0.65, suggesting that the risk model possesses some diagnostic significance.The risk curve provided insights into the association between risk scores and the survival status of BC patients. Our analysis revealed that the high-risk group exhibited a higher mortality rate compared to the low-risk group. Furthermore, the heatmap showed the differential expression of 5 genes in different risk groups(Figure 3C&F).In TCGA-BC, we conducted GSEA enrichment analysis on genes in the high-low risk group, and the top 5 items in the GO annotation were as follows: ENERGY DERIVATION BY OXIDATION OF ORGANIC COMPOUNDS, CELLULAR RESPIRATION, GENERATION OF

PRECURSOR METABOLITES AND ENERGY, RESPIRATORY ELECTRON TRANSPORT CHAIN and ELECTRON TRANSPORT CHAIN.Besides, the top 5 KEGG pathways were OXIDATIVE PHOSPHORYLATION, PARKINSONS DISEASE, HUNTINGTONS DISEASE, ALZHEIMERS DISEASE, and CARDIAC MUSCLE CONTRACTION, as shown in Figure 3G&H. As shown in Figure 3I, the KEGG analysis conducted using the R package "GSVA" revealed several enrichment pathways, including FOLATE_BIOSYNTHESIS, PYRUVATE_METABOLISM, OXIDATIVE_PHOSPHORYLATION,TGF_BETA_SIGNALING_PATHWAY, GNRH_SIGNALING_PATHWAY,FC_EPSILON_RI_SIGNALING_PATHWAY, RENAL_CELL_CARCINOMA, and VEGF_SIGNALING_PATHWAY.

3.4 Genetic variation analysis

The analysis of Figure 4A&B showed that there were differences in the TOP10 genes with high mutation frequency (such as *TP53*, *TTN*, *CDH1*, etc.) and there was no statistically significant difference in TMB between the high and low-risk group (P= 0.96). Based on TCGA-BC, the CNV variation frequency of the high-low risk group was analyzed using GISTIC 2.0, as shown in Figure 4C&D, we found no significant difference in the frequency of CNV variation in different risk groups.

3.5 Immune microenvironment and immunotherapy prediction

Initially, we employed the wilcox.test to compare the relative abundance of immune cells in high- and low-risk groups. The results indicated that there were no significant differences between the high and low-risk groups in immune cells including

Activated_CD4_T_cell, Effector_memory_CD4_T_cell, Memory_B_cell, Type_2_T_helper_cell, and Immature_dendritic_cell. However, significant differences were observed in the remaining 24 types of immune cells ($p< 0.05$), as illustrated in Figure 5A. As shown in Figure 5B, the StromalScore, ImmuneScore and ESTIMATE score of the high-risk group were lower than those of the low-risk group ($p< 0.001$), indicating that tumor purity was higher than in the low-risk group ($p<0.001$). To assess the potential impact of immune checkpoints on blocking therapy, we conducted a further analysis to examine the expression of various immune checkpoints, including *BTLA*, *TNFSF4*, *CD276*, *CD28*, *CD48*, *CD40LG*, *CD200R1*, *HLLA2*, *IDO2*, and *TNFSF15*. The result, as depicted in Figure 5C, demonstrated that *TNFSF15* and *TNFSF4* did not exhibit significant differences. However, significant variations were observed in the expression levels of the other genes between the high and low-risk groups.

3.6 Prediction of potential drugs targeting BC

We utilized the CTD database to individually search for *PSMD10*, *PSMD14*, *PSMD2*, *PSME1*, and *PSME2* in order to construct the biomarker-drug interaction network. Subsequently, we visualized the result. As illustrated in Figure 6, a total of 252 drug molecules were predicted based on the 5 biomarkers.

3.7 Construction of a nomogram

Univariate and multivariate Cox regression analysis was used to determine whether

risk score was an independent prognostic factor for BC patients. The analysis found that age, stage and risk type were independently correlated with prognosis, indicating that risk score was an independent prognostic factor for BC patients, as shown in Figure 7A. We developed a nomogram model incorporating age, stage, and risk type to predict the 1, 2, and 3-year OS of BC patients. The analysis revealed that all three factors have reliable predictive abilities. Furthermore, we employed calibration curves to confirm the consistency between the actual and predicted values. The results indicated high accuracy of the risk score, as depicted in Figure 7B-E. Subsequent ROC analysis showed that the AUC of 1-year, 2-year, and 3-year tests were 73.9, 73.5, and 69.2, respectively, indicating that the nomogram model had high accuracy for BC, as shown in Figure 7F-H.

3.8 RT-qPCR

We used RT-qPCR to analyze the differential expression of 5 biomarkers in BC tissues and adjacent tissues, and the results were shown in Figure 8. Compared with adjacent tissues, these 5 biomarkers were highly expressed in BC.

4. DISCUSSION

BC is the leading cause of malignant tumors in women, presenting a significant health concern. The majority of BC cases lack symptoms in the early stages, making it

challenging to detect. As the incidence of BC continues to rise, particularly among younger individuals, early detection, diagnosis, and treatment are crucial for improving patient outcomes and quality of life[12]. Polyamines, essential metabolites for cell proliferation, have been found to be elevated in cancer[13]. Increasingly, studies are uncovering the involvement of polyamine metabolism in tumor development, shedding light on potential therapeutic targets and strategies.In this study, the transcriptome sequencing data from TCGA-BC was analyzed, focusing on polyamine metabolism. Initially, the expression profile of TCGA-BC was divided into two subtypes, C1 and C2, revealing significant differences in survival between the two groups. Subsequently, five biomarkers, namely *PSMD10*, *PSMD14*, *PSMD2*, *PSME1*, and *PSME2*, were identified as potential prognostic markers for BC.Additionally, a risk model was constructed, demonstrating that the high-risk group had lower OS. Gene mutation did not directly correlate with different risk groups. Furthermore, Immunoinfiltration analysis revealed significantly different immune cells in different risk groups.A total of 252 drug molecules were predicted by five biomarkers, and nomogram was constructed to predict the accuracy of the risk scoring model for the diagnosis of BC.

In recent years, with the continuous development of transcriptome sequencing, more and more bioinformatic analyses have revealed diagnostic biomarkers for BC. For example, Liu S et al. found that targeting lncROPM-*PLA2G16* may be a new treatment for BC[14]. Apoptoses-related prognostic marker genes *CISD1* and *GPX4*

can be used as biomarkers to predict the prognosis of BC patients[15]. Pei S et al. revealed that SM-related genes are associated with tumor progression and immunity in BC patients[16]. In this study, the biomarkers related to the prognosis of BC that were screened were *PSMD10*, *PSMD14*, *PSMD2*, *PSME1*, and *PSME2*, respectively. At present, many studies have revealed the role of these five biomarkers in tumors, including BC. For example, Wang C et al. found that *Hsa-miR-1248* inhibits *PSMD10* and plays a tumor suppressive role in colorectal cancer[17]. Mulla SW et al. revealed the key role of *PSMD10* as an oncoprotein in tumorigenesis[18]. Xuan DTM et al reported that *PSMD10* expression in BC tissues was higher than that in normal tissues[19]. For *PSMD14*, Yang P et al. revealed a novel positive feedback loop between *PSMD14* and ERα signaling in BC[20]. In addition, Lee HJ et al. reported that *PSMD14* induces apoptosis of BC cells by inducing proteasome inhibition[21]. However, *PSMD2* regulated the proliferation of BC cells by regulating p21 degradation[22]. Tian R et al. also found that *PSMD2* is closely related to the progression of BC[23]. Regarding the relationship between *PSME1* and BC, only Yang Y et al. identified *PSME1* as a prognostic gene in breast invasive ductal carcinoma[24]. However, Wu C et al. reported that *PSME2* can recognize immune heat tumors in BC[25]. Dong M et al. successfully screened out prognostic markers of BC, including *PSME2*, *ULBP2*, *IGHE*, etc[26]. Combined with previous findings, our study further complements the importance of these biomarkers for the diagnosis and treatment of BC.Each identified gene plays a pivotal role in the onset and progression of BC, emphasizing the need for molecular mechanism studies to elucidate their specific

actions. While this aspect is not covered in the current study, the identified biomarkers offer a crucial theoretical foundation for the clinical diagnosis of BC patients.Tumor development occurs under the influence of the immune system, and tumor cells have the ability to modulate the immune microenvironment within the tumor tissue, leading to a state of immunosuppression. Furthermore, certain key immune cells also contribute to the progression of tumors.In this study, we found significant differences in all 24 types of immune cells in high/low risk BC patients, including Activated B cell, Regulatory T cell, Type_1_T_helper_cell, Activated_dendritic_cell, Eosinophil, Mast_cell, and Macrophage. Macrophages have a dual potential in cancer. Macrophages have the potential to kill tumor cells, cause vascular damage and tumor necrosis, and activate tumor resistance mechanisms. Instead, in most established tumors, macrophages promote cancer progression and metastasis through a variety of mechanisms. The relationship between macrophages and BC has been reported in many literatures.For example, Li H et al. found that HLF regulates the development of triple-negative BC and chemotherapy resistance by activating macrophages[27]. Chen Y et al showed that tumor recruited M2 macrophages promote BC metastasis through *CHI3L1* protein[28]. Other studies have found that lipid-associated macrophages in the tumor microenvironment can promote BC progression[29]. The results of these researchers have demonstrated that macrophages play a key role in regulating the malignant development of BC. In this study, we also further revealed the potential function of macrophages, which contributed to improving the prognosis of BC patients.

In summary, our study has identified 5 crucial biomarkers - *PSMD10*, *PSMD14*, *PSMD2*, *PSME1*, and *PSME2* - with significant potential for diagnosing BC in patients. Furthermore, the differential immune cells we have identified offer valuable insights for further exploration into the malignant progression of BC. However, it is important to note that our paper lacks corresponding clinical validation and experimental studies, highlighting the need for further refinement and improvement in future research endeavors.

ACKNOWLEDGEMENTS

Thanks to everyone who contributes to this article.

FUNDING

The authors declare that no financial support was received for the research, authorship, and/or publication of this article.

AVAILABILITY OF DATA AND MATERIALS

The data that support the finding of this study are available from the TCGA database(https://xenabrowser.net), METABRIC and MSigDB database. The original contributions presented in the study are included in the article; further inquiries can be directed to the corresponding authors.

AUTHORS' CONTRIBUTIONS

XZ and WX designed the study and wrote the first draft of the manuscript. HG and XL conducted research. HM participated in data analysis. WT and XM revised the manuscript. All authors read and approved the final manuscript.

ETHICS APPROVAL AND CONSENT TO PARTICIPATE

All protocols were approved by Ethics Committee of Xinqiao Hospital, Army Medical University(Chongqing, China) and written informed consent was provided by all participants.

PATIENT CONSENT FOR PUBLICATION

All patients involved in the present study consented to the publication of their data.

COMPETING INTERESTS

The authors declare no confict of interest.

5. REFERENCES

[1] BARZAMAN K, KARAMI J, ZAREI Z, et al. Breast cancer: Biology, biomarkers, and treatments [J]. International immunopharmacology, 2020, 84: 106535.

[2] MORROW M. Identification and management of the woman at increased risk for breast cancer development [J]. Breast cancer research and treatment, 1994, 31(1): 53-60.

[3] KOLAK A, KAMIŃSKA M, SYGIT K, et al. Primary and secondary prevention of breast cancer [J]. Annals of agricultural and environmental medicine : AAEM, 2017, 24(4): 549-53.

[4] KIM M Y. Breast Cancer Metastasis [J]. Advances in experimental medicine and biology, 2021, 1187: 183-204.

[5] LEV S. Targeted therapy and drug resistance in triple-negative breast cancer: the EGFR axis [J]. Biochemical Society transactions, 2020, 48(2): 657-65.

[6] DAMIANI E, WALLACE H M. Polyamines and Cancer [J]. Methods in molecular biology (Clifton, NJ), 2018, 1694: 469-88.

[7] THOMAS T, THOMAS T J. Polyamines in cell growth and cell death: molecular mechanisms and therapeutic applications [J]. Cellular and molecular life sciences : CMLS, 2001, 58(2): 244-58.

[8] CONI S, BORDONE R, IVY D M, et al. Combined inhibition of polyamine metabolism and eIF5A hypusination suppresses colorectal cancer growth through a converging effect on MYC translation [J]. Cancer letters, 2023, 559: 216120.

[9] NOVITA SARI I, SETIAWAN T, SEOCK KIM K, et al. Metabolism and function of polyamines in cancer progression [J]. Cancer letters, 2021, 519: 91-104.

[10] KAMINSKI L, TORRINO S, DUFIES M, et al. PGC1α Inhibits Polyamine Synthesis to Suppress Prostate Cancer Aggressiveness [J]. Cancer research, 2019, 79(13): 3268-80.

[11] MENDEZ R, KESH K, ARORA N, et al. Microbial dysbiosis and polyamine metabolism as predictive markers for early detection of pancreatic cancer [J]. Carcinogenesis, 2020, 41(5): 561-70.

[12] ZHANG Y N, XIA K R, LI C Y, et al. Review of Breast Cancer Pathologigcal Image Processing [J]. BioMed research international, 2021, 2021: 1994764.

[13] HOLBERT C E, CULLEN M T, CASERO R A, JR., et al. Polyamines in cancer: integrating organismal metabolism and antitumour immunity [J]. Nature reviews Cancer, 2022, 22(8): 467-80.

[14] LIU S, SUN Y, HOU Y, et al. A novel lncRNA ROPM-mediated lipid metabolism governs breast cancer stem cell properties [J]. Journal of hematology & oncology, 2021, 14(1): 178.

[15] WANG D, WEI G, MA J, et al. Identification of the prognostic value of ferroptosis-related gene signature in breast cancer patients [J]. BMC cancer, 2021, 21(1): 645.

[16] PEI S, ZHANG P, YANG L, et al. Exploring the role of sphingolipid-related genes in clinical outcomes of breast cancer [J]. Frontiers in immunology, 2023, 14: 1116839.

[17] WANG C, WANG B, LIANG W, et al. Hsa-miR-1248 suppressed the proliferation, invasion and migration of colorectal cancer cells via inhibiting PSMD10 [J]. BMC cancer, 2022, 22(1): 922.

[18] MULLA S W, VENKATRAMAN P. Novel Nexus with NFκB, β-catenin, and RB1 empowers PSMD10/Gankyrin to counteract TNF-α induced apoptosis establishing its oncogenic role [J]. The international journal of biochemistry & cell biology, 2022, 146: 106209.

[19] XUAN D T M, WU C C, KAO T J, et al. Prognostic and immune infiltration signatures of proteasome 26S subunit, non-ATPase (PSMD) family genes in breast cancer patients [J]. Aging, 2021, 13(22): 24882-913.

[20] YANG P, YANG X, WANG D, et al. PSMD14 stabilizes estrogen signaling and facilitates breast cancer progression via deubiquitinating ERα [J]. Oncogene, 2024, 43(4): 248-64.

[21] LEE H J, LEE D M, SEO M J, et al. PSMD14 Targeting Triggers Paraptosis in Breast Cancer Cells by Inducing Proteasome Inhibition and Ca(2+) Imbalance [J]. International journal of molecular sciences, 2022, 23(5).

[22] LI Y, HUANG J, ZENG B, et al. PSMD2 regulates breast cancer cell proliferation and cell cycle progression by modulating p21 and p27 proteasomal degradation [J]. Cancer letters, 2018, 430: 109-22.

[23] TIAN R, TIAN J, ZUO X, et al. RACK1 facilitates breast cancer progression by competitively inhibiting the binding of β-catenin to PSMD2 and enhancing the stability of β-catenin [J]. Cell death & disease, 2023, 14(10): 685.

[24] YANG Y, LUO D, GAO W, et al. Combination Analysis of Ferroptosis and Immune Status Predicts Patients Survival in Breast Invasive Ductal Carcinoma [J]. Biomolecules, 2023, 13(1).

[25] WU C, ZHONG R, SUN X, et al. PSME2 identifies immune-hot tumors in breast cancer and associates with well therapeutic response to immunotherapy [J]. Frontiers in genetics, 2022,

13: 1071270.

[26] DONG M, CUI X, WANG G, et al. Development of a prognostic signature based on immune-related genes and the correlation with immune microenvironment in breast cancer [J]. Aging, 2022, 14(13): 5427-48.

[27] LI H, YANG P, WANG J, et al. HLF regulates ferroptosis, development and chemoresistance of triple-negative breast cancer by activating tumor cell-macrophage crosstalk [J]. Journal of hematology & oncology, 2022, 15(1): 2.

[28] CHEN Y, ZHANG S, WANG Q, et al. Tumor-recruited M2 macrophages promote gastric and breast cancer metastasis via M2 macrophage-secreted CHI3L1 protein [J]. Journal of hematology & oncology, 2017, 10(1): 36.

[29] LIU Z, GAO Z, LI B, et al. Lipid-associated macrophages in the tumor-adipose microenvironment facilitate breast cancer progression [J]. Oncoimmunology, 2022, 11(1): 2085432.

TABLES

Table 1 Primer sequence

Gene	F(5'-3')	R(5'-3')	Length(bp)
PSMD10	CTGACCAGGACAGCAGAACTGC	CTTGAGCACCTTTTCCCAGAAGG	189
PSMD14	GCTATGCCACAGTCAGGAACAGG	ACAAGGCTTCAAAGCTCTGCTGAG	190
PSMD2	GACAAGGACAAAGAACAGGAGCTG	CCTTCAGTTTGCCATAGTGTGGAC	211
PSME1	GTACCAAGACAGAGAACCTGCTCG	TCAGGCACTGGGATGTCCAATG	136
PSME2	CTCCACCCAAGGATGATGAGATG	CACCTTCTCCTGGATTGCTACC	227
GAPDH	GGAGCGAGATCCCTCCAAAAT	GGCTGTTGTCATACTTCTCATGG	197

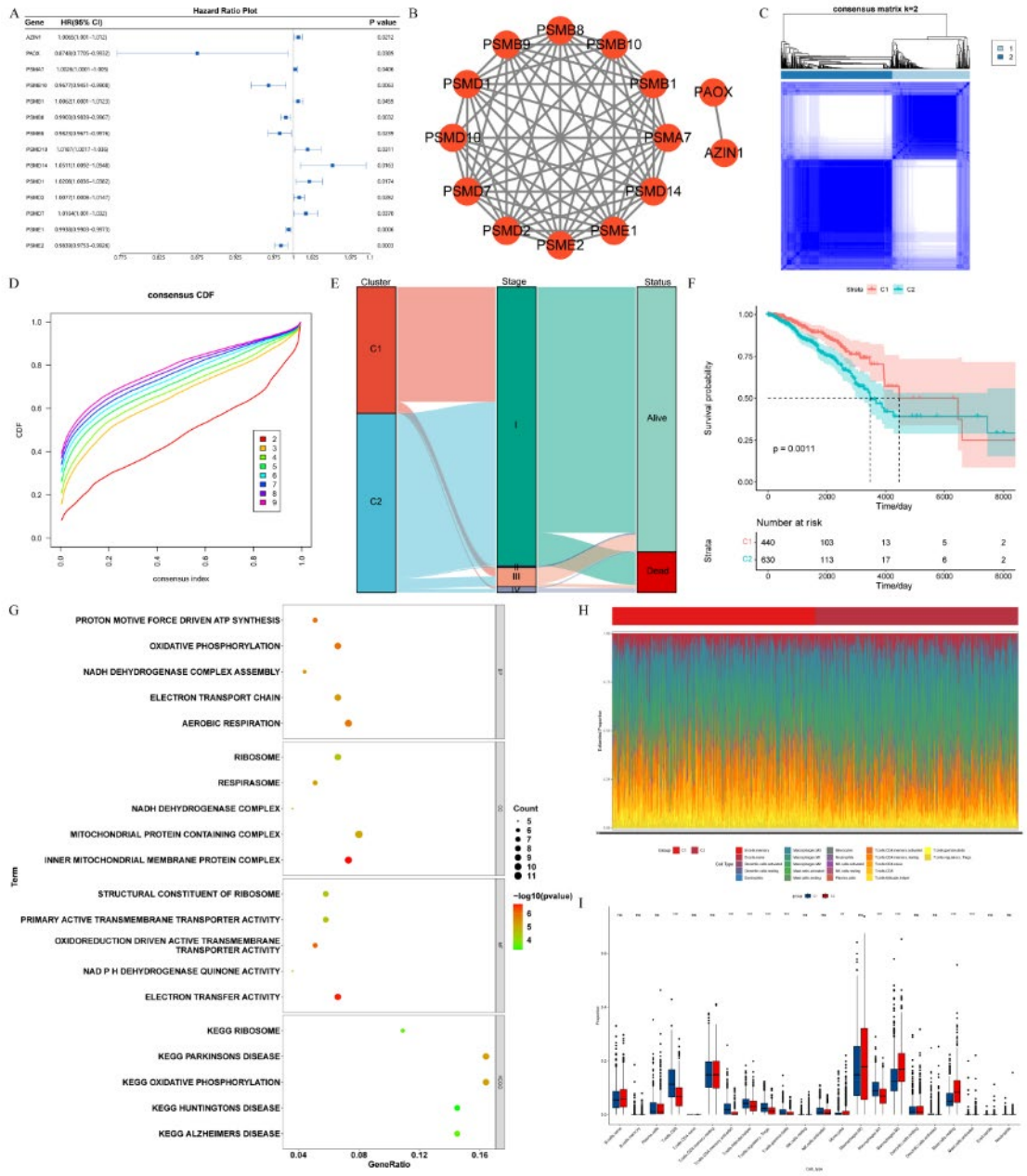

Figure 1 Differentiation of BC polyamine metabolic subtypes. (A)Risk ratio forest plot; (B)PPI network;(C) Clustering heatmap;(D) Cumulative distribution function graph;(E) Sankey diagram;(F) Survival analysis of C1 and C2;(G) Functional annotation of TOP5 differential genes in two subtypes;(H-I) The proportion of 22 kinds of immune cells in different groups.

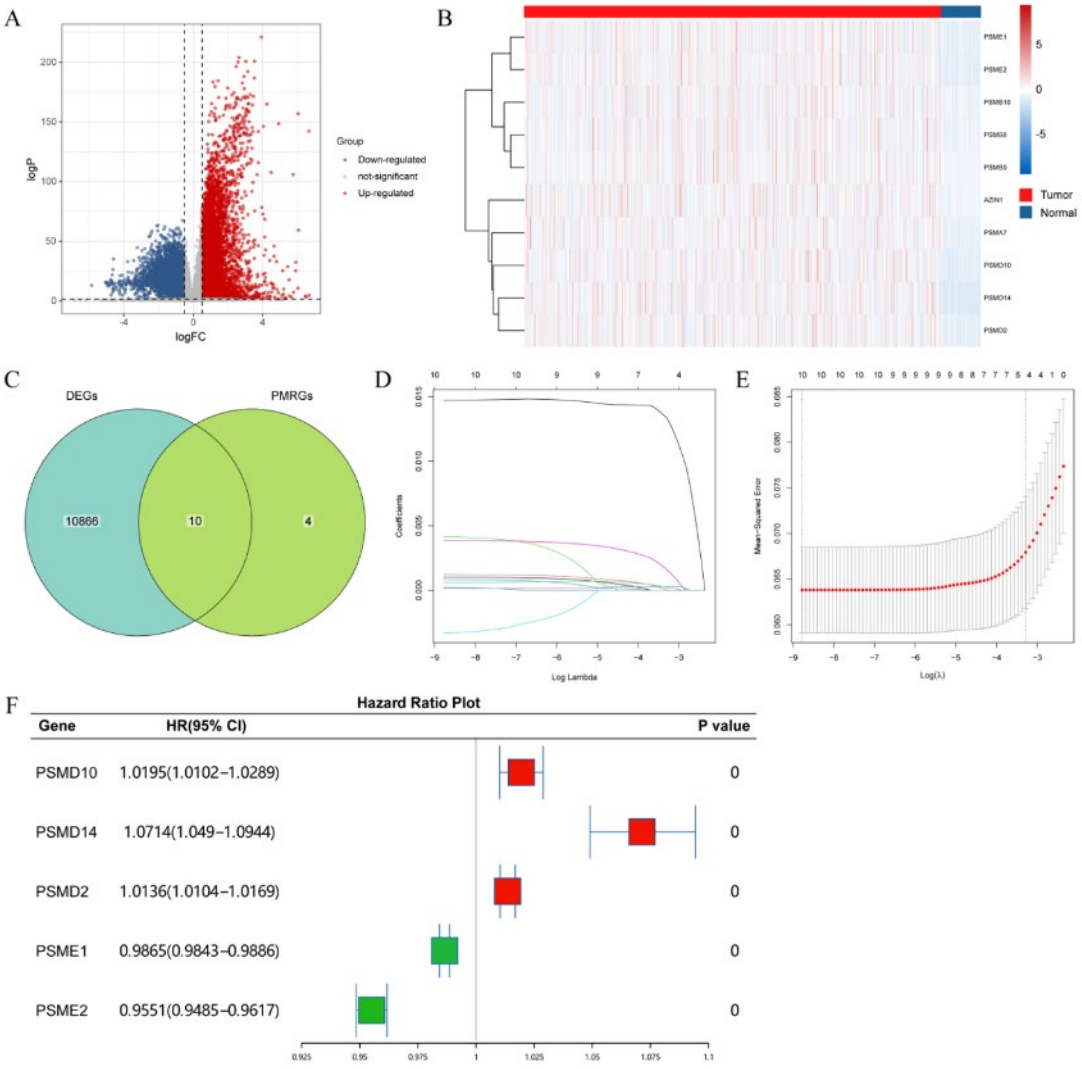

Figure 2 Identification of prognostic associated PMRGs in BC. (A) Volcano plot; (B)Heatmap;(C) Venn diagram of prognostically related PMRGs;(D-E) LASSO regression analysis;(F)Forest map.

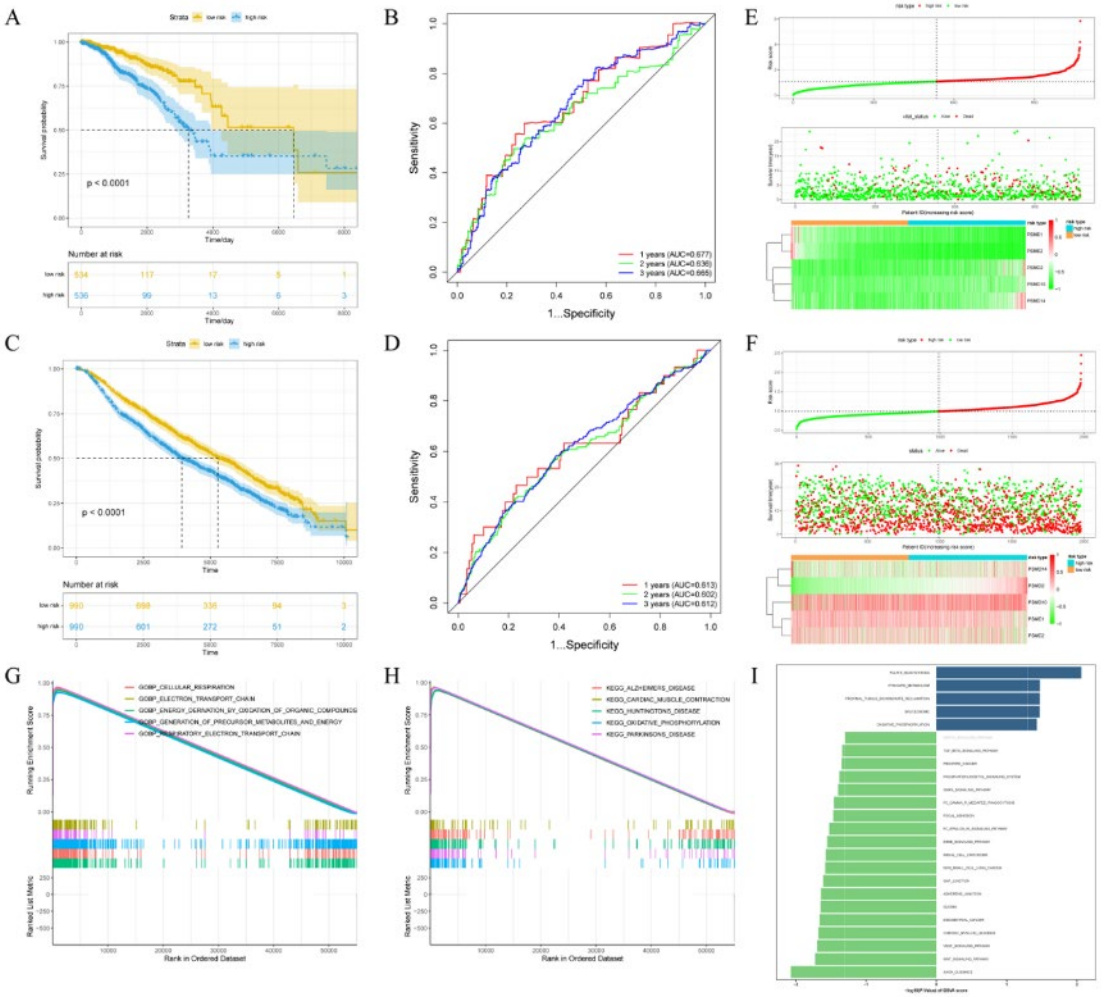

Figure 3 Construction and verification of risk model. (A) Kaplan-Meier survival analysis of patients in training set; (B) ROC curve of patients in training set;(C)Kaplan-Meier survival analysis of patients in validation set;(D) ROC curve of patients in validation set;(E) Risk curve in training set;(F) Risk curve in validation set;(G) GSEA result in training set;(H) GSEA result in validation set;(I)GSVA enrichment analysis.

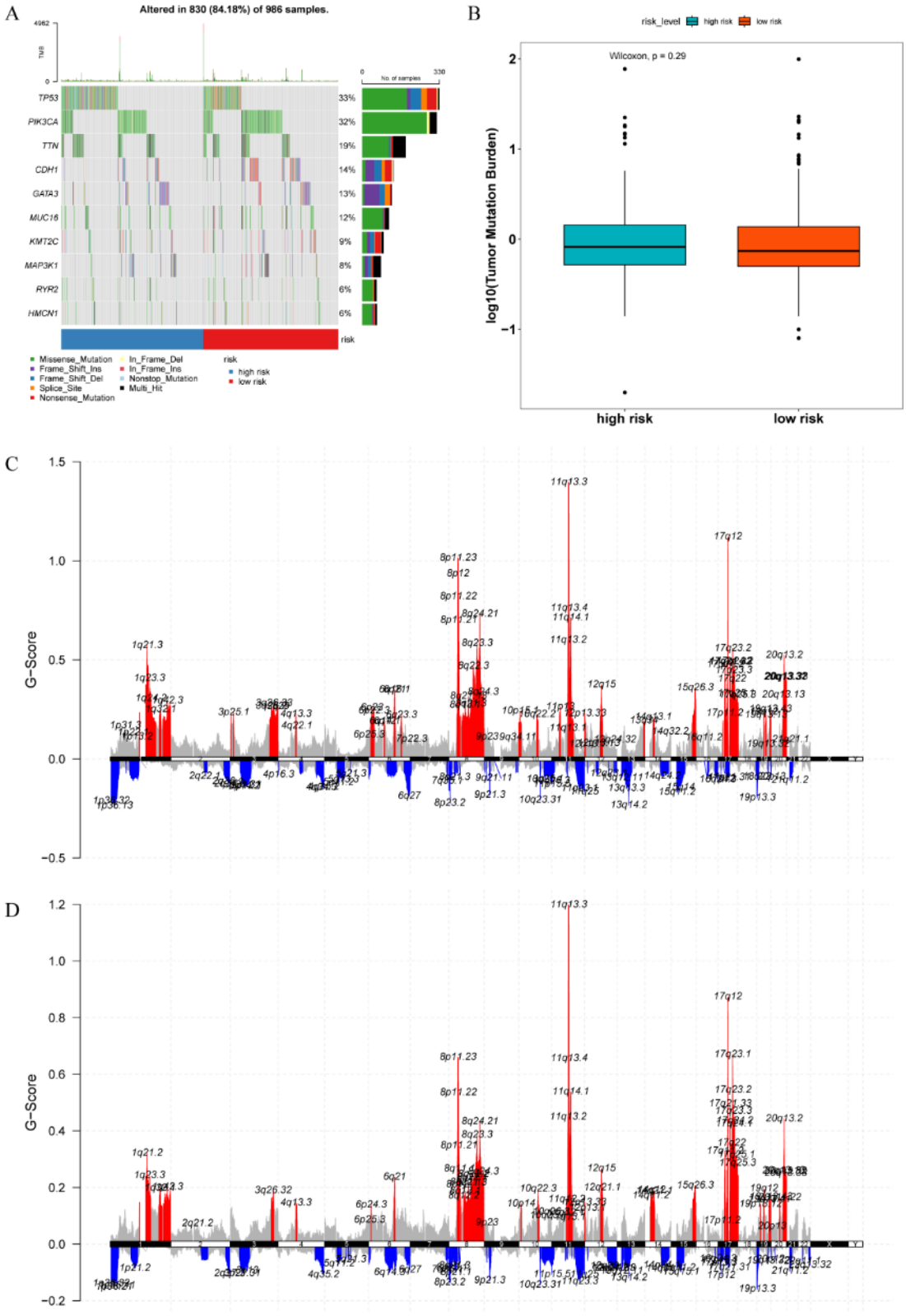

Figure 4 Mutation load and CNV analysis. (A-B) Analysis of tumor mutation load; (C) CNV mutation in high - and low-risk groups.

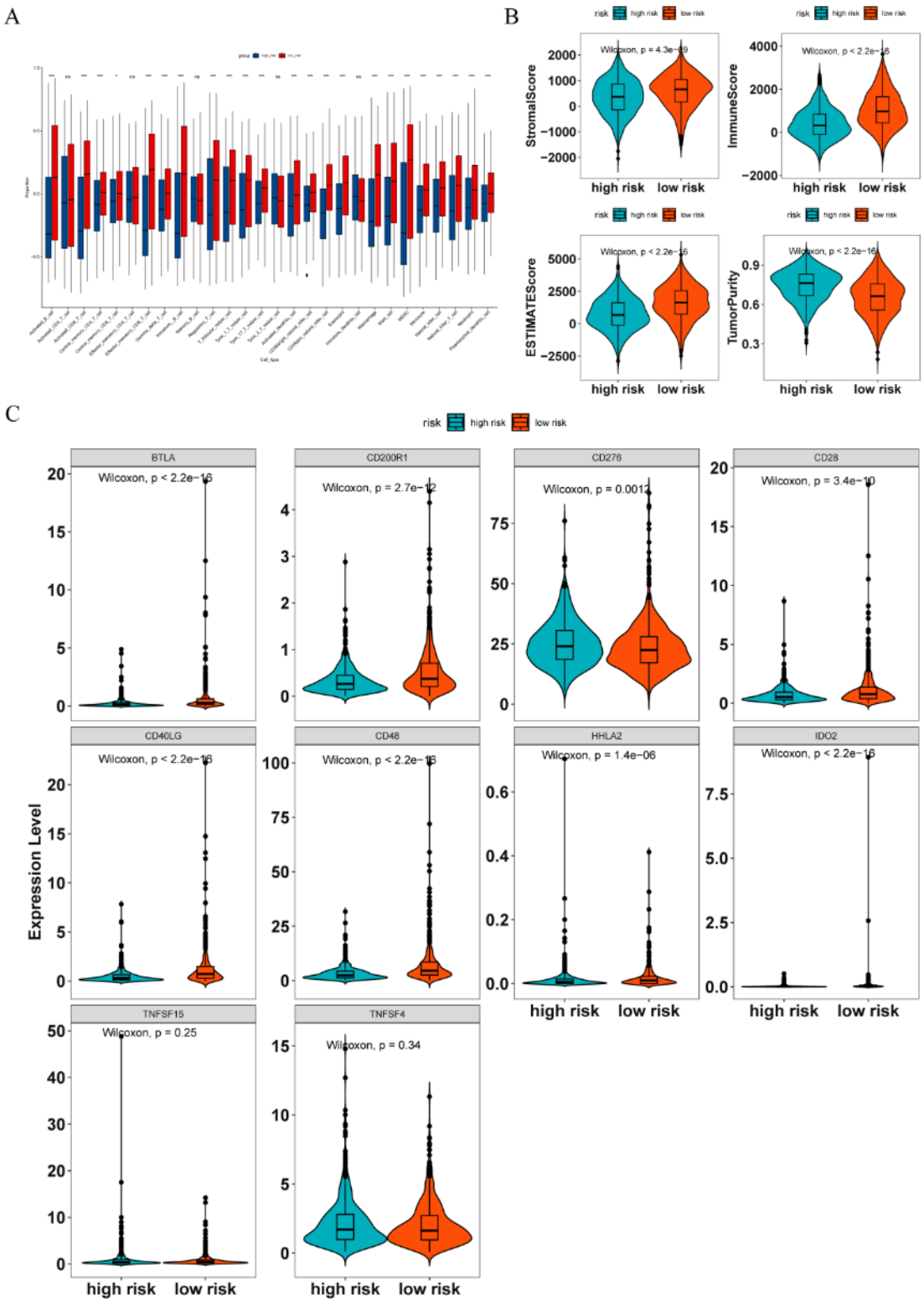

Figure 5 Immune microenvironment and immunotherapy prediction.(A)Difference boxplot of immunoinfiltration between high and low risk groups; (B) Tumor purity analysis;(C)Violin diagram of differences in immune checkpoint genes in high and low risk groups.

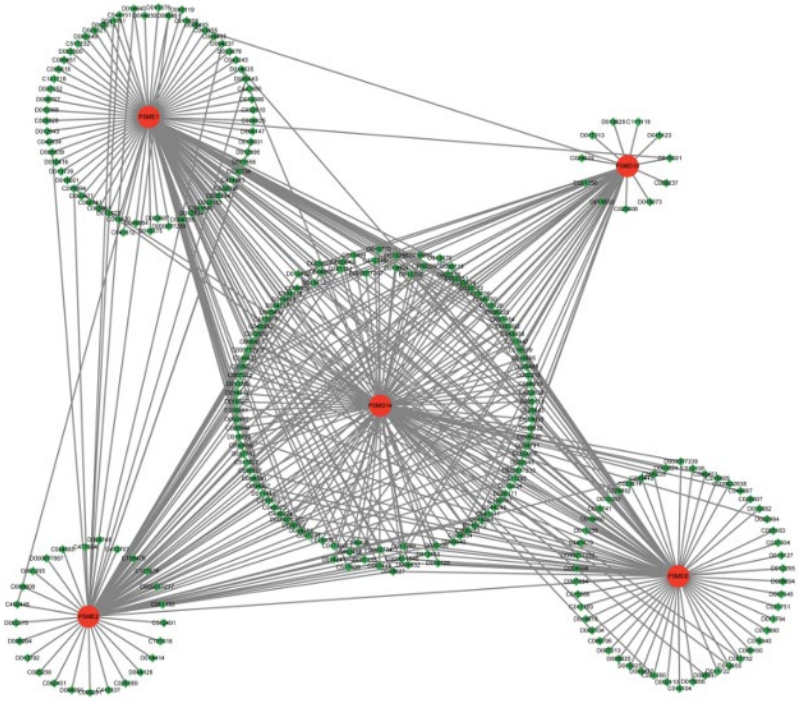

Figure 6 Biomarker-drug molecule interaction network.

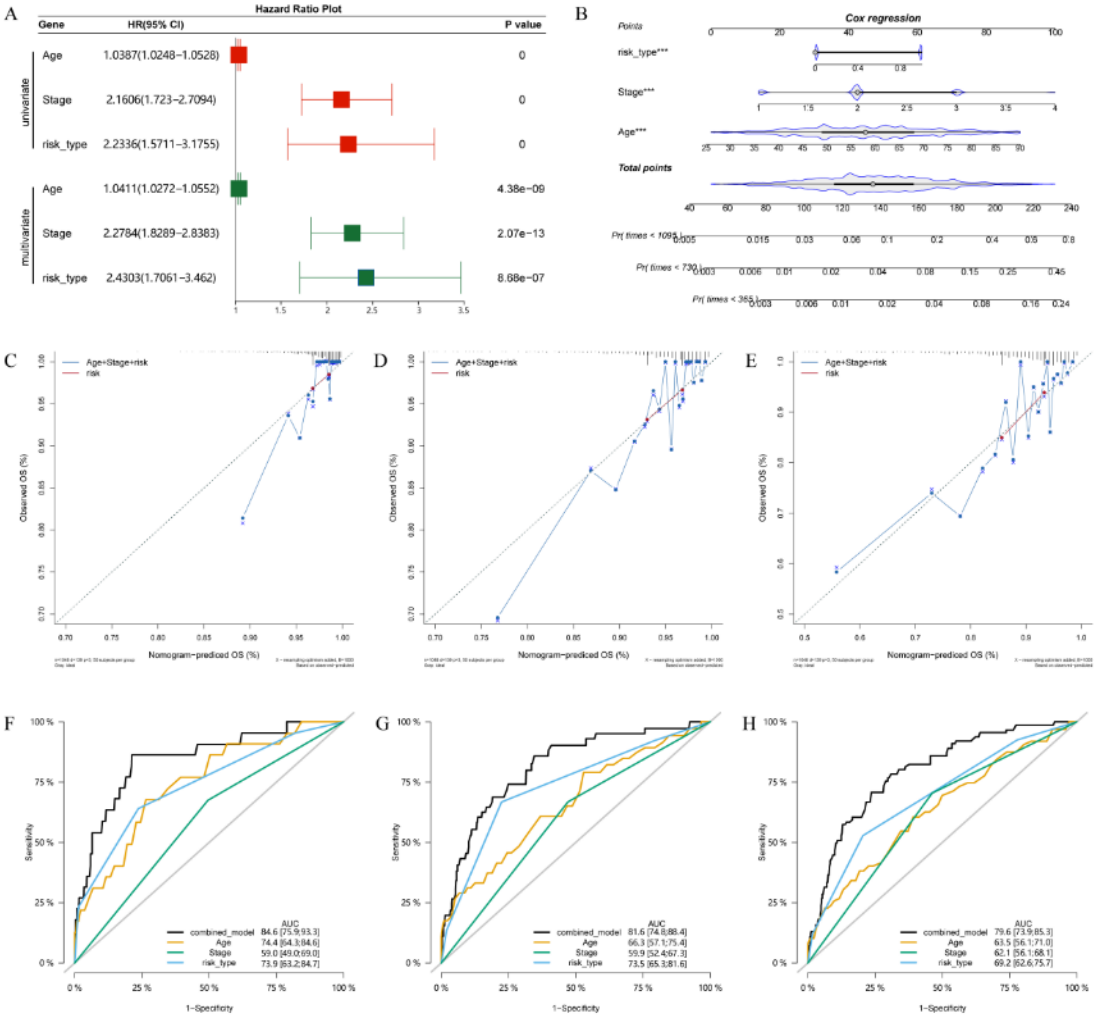

Figure 7 Nomogram model.(A) Univariate and multifactorial independent prognostic analysis; (B) Prognosis nomogram;(C-E) Calibration curves for 1, 2 and 3 years;(F-H) Prognostic ROC curve.

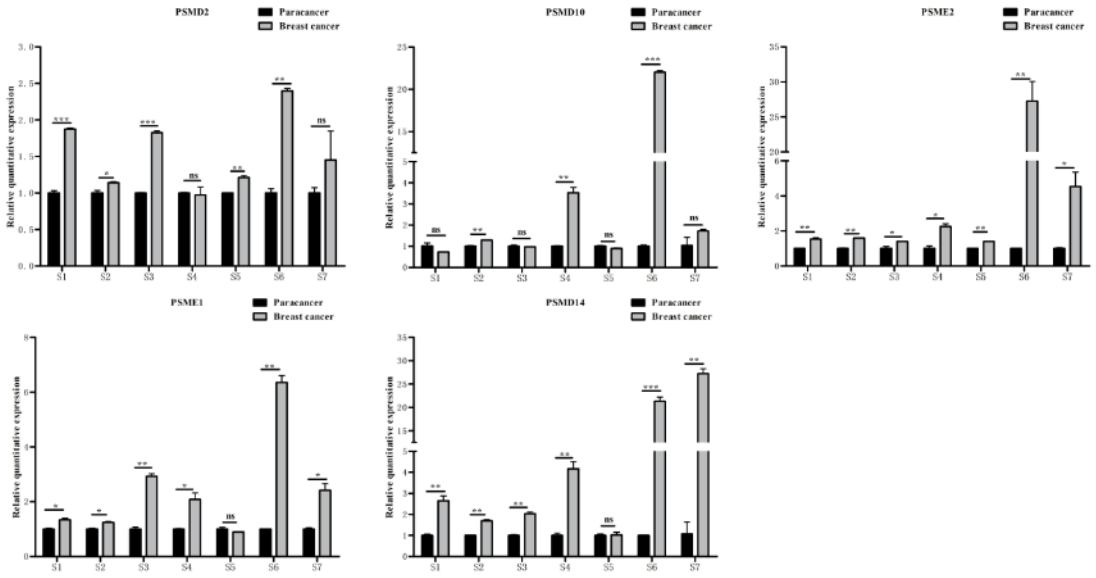

Figure 8 The expression of 5 biomarkers in BC and adjacent tissues was analyzed by RT-qPCR.

Corresponding Author:

Weidong Xiao

Department of General Surgery, Xinqiao Hospital, Army Medical University, 83 Xinqiao Zhengjie, Chongqing, 400037, China

E-mail: xiaoweidong@tmmu.edu.cn

Xiaolong Li

Department of General Surgery, Xinqiao Hospital, Army Medical University, 83 Xinqiao Zhengjie, Chongqing, 400037, China

E-mail: 917304077@qq.com